Novel Optimal Dispatch Method for Multiple Energy Sources in Regional Integrated Energy Systems Considering Wind Curtailment

Yang Gao, *Member*, *IEEE*, and Qian Ai, *Senior Member*, *IEEE*

***Abstract*—Power-to-gas technology uses temporary surplus electricity to create either renewable hydrogen or renewable natural gas, which can then be stored in natural-gas pipelines and used when needed. As a result, P2G transforms conventional one-way coupling of a power/heat/natural-gas system into two-way coupling. Furthermore, its operating characteristics makes it possible to more effectively utilize wind-power. This paper describes a new optimal dispatch model for integrated electricity/gas/heat energy systems. The model considers the effective use of surplus wind-energy with electricity-to-gas equipment. First, a multi-energy network model is built, taking into account both equipment and network constraints. Then, we apply a novel two-layer optimization method, which uses P2G, to "absorb" wind power. While the top-layer model is used for the day-ahead dispatch of the natural-gas network containing P2G, the bottom-layer model describes the day-ahead economic dispatch of the electricity/heat system, which includes wind power. Based on the Karush-Kuhn-Tucher conditions of the bottom-layer model, the two-layer model is transformed into a single-layer model, and we linearize the nonlinear equation to convert the nonlinear model into a mix-integer linear programming problem, which is solvable using the General Algebraic Modeling System. Finally, numerical case-studies are performed to evaluate the accuracy and effectiveness of the proposed method.**

***Index Terms*—Multi-enery coupling, power-to-gas, two-layer optimization, wind-power consumption.**

NOMENCLATURE

A. Abbreviations

P2G	Power to gas.
IES	Integrated energy system.
PSO	Particle swarm optimization.
MT	Micro gas turbine.
RIES	Regional integrated energy system.
KKT	Karush-Kuhn-Tucher.
GAMS	General algebraic modeling system.
MT	Micro-gas turbine.
SNG	Synthetic natural gas.
GSF	Generation shift factor.
WT	Wind turbine.
TP	Thermal power.
DG	Distributed generator.
MILP	Mix-integer linear programming problem.

B. Indices

t	Index of hour.
k	Index of unit.
l	Index of transmission line.
i	Index of electrical node.
m	Index of gas node.
N	Index of electrical node.
$\phi_{\rm hs}, \phi_{\rm ex}$	Index set of heat source and heat-exchanger.
$\phi_{\rm heat}$	Index set of lines of the heat network.

C. Parameters

$W_{i,t}$	Gas well supply of node i (kcf).
$L_{i,\rm gas,t}$	Gas load of MT (kcf).
η_{ij}	Pipeline flow rate.
σ_i	Node pressure of natural gas pipeline (Pa).
C_{ij}	Pipeline constant.
n_g	Number of natural gas nodes.
$P_{\rm psr}$	Compressor power consumption (kcf).
$L_{\rm psr}$	Compressor electric load (kW).
$\zeta_{\rm psr}$	Conversion efficiency of compressor.
$H_{k,t,hs}$	Heat output of heat source (kW).
C	Specific heat capacity of water (kJ/(kg·°C)).
$m_{k,hs}$	Mass flow rate of heat source.
$T_{k,t,\rm hs\_sup}$, $T_{k,t,\rm hs\_ret}$	Mass flow temperature of the supply/return water pipeline at heat-source (K).
$H_{k,t,ex}$	Heat output of heat-exchange station (kW).
$T_{k,t,\rm ex\_sup}$, $T_{k,t,\rm ex\_ret}$	Mass flow temperature of the supply/return water pipeline at heat-exchange station (K).
$T_{k,t,\rm s\_out}$, $T_{k,t,\rm s\_in}$	Mass flow temperature at inlet/ outlet of supply water pipeline (K).
$\alpha_{kt}, T_{am,t}$	Heat loss coefficient and ambient temperature.
$E_{\rm P2G},t,\rm gas$	P2G energy (kW).
$V_{\rm P2G},t,\rm gas$	Gas volume generated by P2G (m^3).
$\eta_{\rm P2G}$	P2G efficiency.
$P_{i,\rm P2G,t}$	Electricity consumption of P2G (kW).
$HHV_{\rm gas}$	High heating value of natural gas.
$\eta_{i,MT}$	Generation efficiency of MT.
$P_{i,\rm MT,t}$	Micro gas turbine output (kW).
$Q_{i,\rm MT\_heat,t}$	Output heat power of MT (kW).

Manuscript received March 12, 2021; revised May 27, 2021; accepted September 7, 2021. Date of online publication January 5, 2022, date of current version June 18, 2023. This work was sponsored by Shanghai Sailing Program (20YF1418800) and Outstanding PhD Graduate Development Scholarship of Shanghai Jiao Tong University.

Y. Gao (corresponding author, email: jjgyxky@126.com) and Q. Ai are with the Key Laboratory of Control of Power Transmission and Conversion, Ministry of Education, Shanghai Jiao Tong University, Shanghai 200240, China.

DOI: 10.17775/CSEEJPES.2021.01780

c_{gi}	Gas well price (\$/kW).
$f_{\text{oper},t}$	Operation cost of lower model (\$).
$c_{i,\text{fire}}$	Grid purchase cost (\$/kW).
$c_{i,\text{wind}}$	Maintenance cost of wind turbine (\$/kW).
$c_{i,\text{curw}}$	Wind curtailment cost (\$/kW).
c_{P2G}	P2G revenue cost (\$/kW).
c_{MT}	Micro gas turbine output cost (\$/kW).
$P_{i,\text{wind},t}$	Wind power output (kW).
$P_{i,\text{fire},t}$	Purchase electricity (kW).
$P_{i,\text{MT},t}$	Micro gas turbine output (kW).
$L_{i,\text{ele},t}$	Electrical load (kW).
$P_{\text{ele},l,\text{lim}}$	Line transmission limit (kW).

I. Introduction

With the increasing proportion of distributed energy sources with high penetration rates, the problems of energy waste and high dispatch costs are becoming more and more critical. The integrated energy system utilizes the complementation of multiple energy sources to significantly improve energy utilization and economic benefits, and meet the needs of power supply, heating, and gas supply [1]–[3]. However, there are still significant differences in the transmission characteristics between various energy subsystems, especially for natural gas networks and thermal networks, which have huge potential for dispatching. In addition, due to the emergence of energy hubs, energy conversion and storage units play a vital role in multi-energy complementation, which enhances the coupling of multi-energy sources and increases the complexity of optimal regulation. Therefore, making use of the flexibility potential of the IES to reduce the operation cost of existing energy equipment is an issue worthy of attention [4]–[6].

At present, domestic and foreign scholars have carried out preliminary research on the optimization of multi-energy complementary of the IES. Scholars at the University of Manchester in the United Kingdom developed an integrated energy user interaction platform to facilitate energy consumption, energy conservation, and user demand-side response [7]–[10]. Paper [11] proposed a joint optimal dispatching method for cooling, heating, and electric power, considering the combination of the safety constraints of the natural gas system and the optimal dispatching model. Paper [12] introduced a thermal energy flow model compatible with the power system, which took into account the constraints of the heat exchange. The authors in [13] used the energy-hub to represent the terminal unit of the integrated energy system, which can be coupled with the power grid, natural gas network and transportation network at the same time. An optimal scheduling strategy was discussed in [14] for an integrated electricity-heat system, which fully considered the characteristics of thermal energy transmission. Paper [15] proposed an incentive-based coordination mechanism for distributed operations of an integrated electricity-heat system to encourage pipeline energy storage utilization and flexibility provisions from the heat network and designed an optimal thermal flow model to reduce complexity. A non-iterative distributed strategy was discussed in [16] based on the dynamic equivalent model, which was used for the integrated operation of electricity and thermal systems, and mapping the internal state of a district heating network to the boundary state. In the above research, electricity-gas-heat energy networks are primarily unidirectionally coupled, and the impact of high-penetration renewable energy, such as wind power, on the operation of the IES is not considered.

In the electric-heat system, in order to improve energy utilization and reduce the operating cost of the heat system, the MT has begun to be widely used. However, due to the limitation of the thermoelectric ratio, how to coordinate the operation of the MT and high-permeability wind power in the grid has become a huge challenge [17]–[19]. While the P2G technology provides a new idea for solving this problem, the P2G can produce natural gas through chemical reactions, thereby realizing the conversion of electric energy to natural gas. To minimize the operating cost of energy hubs including P2G, paper [20] proposed a day-ahead dispatching scheme for an IES with the two-way flow of energy. In the low valley hours, P2G is used to convert cheap electricity into natural gas to reduce the natural gas purchase cost. The classic particle swarm algorithm is used to solve the joint planning problem, including the MT and P2G, but neglecting the nonlinear constraints [21], [22]. A day ahead dispatching model considering the dynamic constraints of the gas pipeline and P2G is proposed to improve the level of wind power consumption. However, the thermal network is not explored [23], [24].

In contrast to the existing studies mentioned above, this paper aims to shed light on the feasibility and economics of the RIES by considering the utilization rate of surplus windpower, where the operation of a wide range of multi-energy technologies need to be optimized. For this purpose, a two-layer robust optimal scheduling method is proposed, taking into account the uncertain characteristics of different multi-energy coupling devices, and a detailed electricity, heat- and gas-network model.

The proposed framework is studied in a multi-energy district that includes a modified IEEE-9-node power-system, a 7-node natural-gas system, and a 6-node thermal system. Different cases for the penetration of P2G storage, various wind curtailment costs, and a comparison between the two-layer- and single-layer-models are presented to highlight the features of this method. The most significant benefits of this paper are:

i) The effects of different wind curtailment costs on wind energy utilization and the power to gas conversion process are fully considered.

ii) Compared with the single-layer model, the natural gas network and electric-thermal network of the double-layer model are considered separately, which fully takes into account the unit cost differences of different energy networks. In the period of no wind curtailment, P2G can produce more natural gas and reduce the operation cost of the whole system.

iii) Based on the KKT condition, the lower-level model is transformed into additional constraints of the upper-level model. By introducing auxiliary variables, the nonlinear constraints are linearized, making the model easier to solve.

The remainder of the paper is structured as follows: Section II discusses the modeling of the IES. The proposed two-layer optimization scheme is described in Section III and

illustrated with a typical RIES in Section IV. The main findings and conclusions are summarized in Section V.

II. Integrated Network Model

As shown in Fig. 1, a two-layer optimization model of the IES is constructed, which includes an electricity/gas/heat load, gas wells, gas pipelines, compressors, wind power, thermal power stations, etc. The day-ahead scheduling model of the electricity-heat network with P2G and wind power is in one layer, considering the costs of grid operations, equipment maintenance and pollutant emission and it is then transformed into the additional constraints of the natural gas system scheduling model in the other layer, according to its KKT conditions. After the nonlinear constraints are linearized, the nonlinear problem is transformed into a mixed integer linear programming problem [25], [26].

A. Natural Gas Network Model

First, build a natural gas network model, including gas source, gas load, node pressure and pipeline flow [27], [28].

1) Gas Well and Load

$$W_{i,\min} \le W_{i,t} \le W_{i,\max} \tag{1}$$

$$L_{i,\text{gas},\min} \le L_{i,gas,t} \le L_{i,\text{gas},\max} \tag{2}$$

2) Pipeline flow

$$\begin{cases} \eta_{ij} = \text{sgn}(\sigma_i, \sigma_j) \times C_{ij}\sqrt{|\sigma_i^2 - \sigma_j^2|} \\ \text{sgn}(\sigma_i, \sigma_j) = \begin{cases} 1, & \sigma_i \ge \sigma_j \\ -1, & \sigma_i < \sigma_j \end{cases} \end{cases} \tag{3}$$

$$\sigma_{i,\min} \le \sigma_i \le \sigma_{i,\max} \tag{4}$$

$$\eta_{ij} = \sum_{m=1}^{n_g} GSF_{\text{gas},m,ij} \times (W_m - L_m) \tag{5}$$

3) Compressor

The compressor can be equivalent to a special transformer with a fixed ratio.

$$P_{\text{psr}} = U \cdot \eta_{ij} \left[\left(\frac{\sigma_i}{\sigma_j} \right)^{\varepsilon} - 1 \right] \tag{6}$$

$$L_{\text{psr}} = P_{\text{psr}} \cdot \zeta_{\text{psr}} \tag{7}$$

B. Heat System Model

1) Heat source

$$H_{k,t,hs} = C \cdot m_{k,hs} \cdot (T_{k,t,\text{hs\_sup}} - T_{k,t,\text{hs\_ret}}), \forall t, \forall k \in \phi_{\text{hs}} \tag{8}$$

2) Heat-exchanger

$$H_{k,t,ex} = C \cdot m_{k,ex}(T_{k,t,\text{ex\_sup}} - T_{k,t,\text{ex\_re}}), \forall t, \forall k \in \phi_{\text{ex}} \tag{9}$$

3) Transmission loss

$$T_{k,t,\text{s\_out}} = T_{am,t} + \alpha_{k,t}(T_{k,t,\text{s\_in}} - T_{am,t}), \forall t, \forall k \in \phi_{\text{heat}} \tag{10}$$

$$T_{k,t,\text{r\_out}} = T_{am,t} + \alpha_{k,t}(T_{k,t,\text{r\_in}} - T_{am,t}), \forall t, \forall k \in \phi_{\text{heat}} \tag{11}$$

C. Electric-heat-gas coupling model

1) P2G

$$E_{\text{P2G},t,\text{gas}} = \eta_{\text{P2G}} \times P_{i,\text{P2G},t} \tag{12}$$

$$V_{\text{P2G},t,\text{gas}} = \frac{E_{\text{P2G},t,\text{gas}}}{HHV_{\text{gas}}} \tag{13}$$

$$0 \le P_{i,\text{P2G},t} \le P_{i,\text{P2G},\max} \tag{14}$$

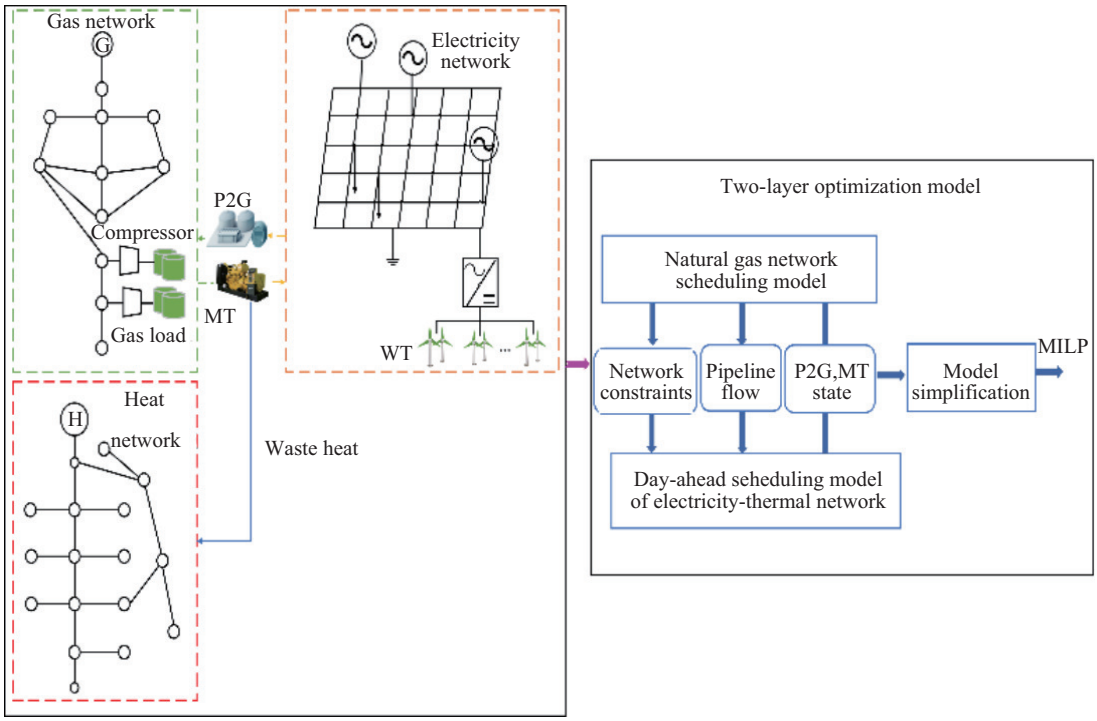

Fig. 1. Two-layer optimization model of the IES.

2) MT

$$\eta_{i,MT} = a_3\left(\frac{P_{i,\mathrm{MT},t}}{P_{i,MT\,\max}}\right)^3 + a_2\left(\frac{P_{i,\mathrm{MT},t}}{P_{i,MT,\max}}\right)^2 + a_1\left(\frac{P_{i,\mathrm{MT},t}}{P_{i,MT,\max}}\right) + a_0 \tag{15}$$

$$Q_{i,\mathrm{MT\_heat},t} = \frac{P_{i,\mathrm{MT},t}}{\eta_{i,MT}}(1-\eta_{i,MT}-\eta_{i,L}) \tag{16}$$

$$0 \le P_{i,\mathrm{MT},t} \le P_{i,MT,\max} \tag{17}$$

III. Two-Layer Optimal Dispatch Method that Considers Wind-power Consumption

A. Optimization: Objectives and Constraints

In the process of multi-energy network regulation, the power network is the fastest, followed by the heat network, and the natural gas network is the slowest. The power network is closely connected with the thermal network through waste heat generated by the MT. Therefore, the electricity-heat network is regarded as one subsystem, and the natural gas network is regarded as another subsystem. In addition, in the case of meeting the constraints of the natural gas network, the random gas load required by the MT in the electricity-heat network is satisfied by optimizing the distribution of the gas source supply. Therefore, the optimal scheduling of the natural gas network is considered in the upper model, while the optimal scheduling of the electricity-heat network is considered in the lower model [29].

1) Upper scheduling model of natural gas network

The upper objective is to minimize the total operation cost of the natural gas network. As the SNG produced by P2G is stored for a long time, its operating cost will not be considered.

$$\textit{Minimize}\ f_{\mathrm{upper}} = \sum_{t=1}^{T}\sum_{i=1}^{n_g}(c_{gi}\times W_{i,t}) \tag{18}$$

s.t. Constraints (1)–(7) and (12)–(17).

2) Lower scheduling model of the electricity-heat network

The objective function in (19) aims to minimize the lower operation cost of the electricity-heat network, where the first four terms are non-MT generation cost, wind turbine quotation, compensation cost for wind curtailments, and the MT generation cost, respectively, while the fifth term represents the P2G revenue cost.

$$\textit{Minimize}\, f_{\mathrm{lower}} = \sum_{t=1}^{T}\sum_{i=1}^{N} f_{\mathrm{oper},t} \tag{19}$$

$$f_{\mathrm{oper},t} = [P_{i,\mathrm{fire},t}\quad P_{i,\mathrm{wind},t}\quad P_{i,\mathrm{curw},t}\quad P_{i,\mathrm{MT},t}\quad L_{i,\mathrm{P2G},t}]\cdot \begin{bmatrix} c_{i,\mathrm{fire}} \\ c_{i,\mathrm{wind}} \\ c_{i,\mathrm{curw}} \\ c_{i,\mathrm{MT}} \\ c_{i,\mathrm{P2G}} \end{bmatrix} \tag{20}$$

$$\textit{s.t.}\ P_{i,\mathrm{fire},t} + P_{i,\mathrm{wind},t} + P_{i,\mathrm{MT},t} = L_{i,\mathrm{ele},t} + P_{i,\mathrm{P2G},t} \tag{21}$$

$$P_{i,\mathrm{DG,min}} \le P_{i,\mathrm{DG},t} \le P_{i,\mathrm{DG,max}} \quad \forall i = 1,\cdots,N, t = 1,\cdots,T \tag{22}$$

$$|GSF_{l-i}\times(P_{i,\mathrm{fire},t} + P_{i,\mathrm{wind},t} + P_{i,\mathrm{MT},t} - L_{i,\mathrm{ele},t} - P_{i,\mathrm{P2G},t}| \le P_{\mathrm{ele},l,\lim} \quad \forall l = 1,\cdots,m \tag{23}$$

Among them, N represents the number of electrical nodes; T represents the scheduling period; m represents the number of lines; $P_{i,\mathrm{DG},t}$ represents the output power of the i^{th} unit at time t; $P_{i,\mathrm{DG,max}}$ are the upper bounds of the DG power and electricity consumption of P2G respectively; $P_{\mathrm{ele},l,\min}$ is the line transmission limit; $\mu_t, \rho_{i,t,\min}, \rho_{i,t,\max}, \pi_{l,t,\min}, \pi_{l,t,\max}$ are the Lagrange multiplier vectors of formals (21)–(23).

B. Model Approach

First, construct the Lagrangian function of the lower model, then convert the lower model into additional constraints of the upper model based on the KKT conditions, and finally, linearize the nonlinear constraints; the specific process is shown in Fig. 2.

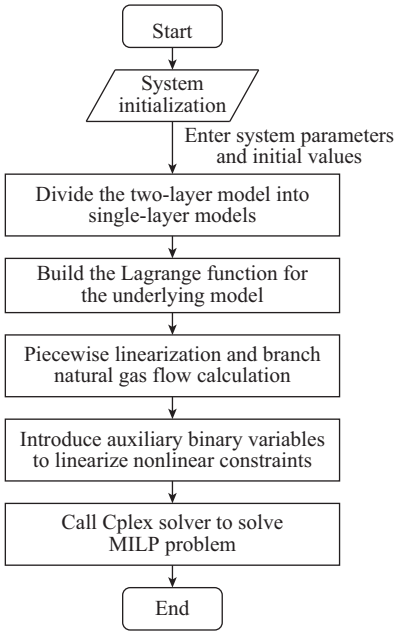

Fig. 2. Two-layer approach.

A Lagrangian function is associated to the lower-level problem (19):

$$\begin{aligned} F = {} & f_{\mathrm{lower}} - \mu_t\Big(\sum_{i=1}^{N} P_{i,\mathrm{fire},t} + P_{i,\mathrm{wind},t} + P_{i,\mathrm{MT},t} \\ & - L_{i,\mathrm{ele},t} - P_{i,\mathrm{P2G},t}\Big) \\ & - \sum_{i=1}^{N}\rho_{i,t,\min}\cdot(P_{i,\mathrm{DG},t} - P_{i,\mathrm{DG,min}}) \\ & - \sum_{i=1}^{N}\rho_{i,t,\max}\cdot(P_{i,\mathrm{DG,max}} - P_{i,\mathrm{DG},t}) \\ & - \sum_{l=1}^{m}\pi_{l,t,\min}[P_{\mathrm{ele},l,\lim} + GSF_{l-i}\times \\ & (P_{i,\mathrm{fire},t} + P_{i,\mathrm{wind},t} + P_{i,\mathrm{MT},t} - L_{i,\mathrm{ele},t} - P_{i,\mathrm{P2G},t})] \\ & - \sum_{l=1}^{m}\pi_{l,t,\max}[P_{\mathrm{ele},l,\lim} - GSF_{l-i}\times \end{aligned}$$

$$(P_{i,\text{fire},t}+P_{i,\text{wind},t}+P_{i,\text{MT},t}-L_{i,\text{ele},t}-P_{i,\text{P2G},t})] \tag{24}$$

Given that the lower-level model is a linear programming problem. The bi-level optimization model can be transformed into a mathematic program with equilibrium constraints by recasting the lower-level model as its KKT optimality condition, then adding them into the upper-level model as a set of additional complimentary constraints.

$$\textit{Maximize -equa. (20)} \tag{25}$$

$$\textit{s.t.}\ \text{Constraints in equa. (1)–(7), (12)–(17), and (21)–(23)} \tag{26}$$

$$0\le\pi_{l,t,\min}\perp[P_{\text{ele},l,\lim}+GSF_{l-i}\times (P_{i,\text{fire},t}+P_{i,\text{wind},t}+P_{i,\text{MT},t}-L_{i,\text{ele},t}-P_{i,\text{P2G},t})]\ge 0 \tag{27}$$

$$0\le\pi_{l,t,\max}\perp[P_{\text{ele},l,\lim}-GSF_{l-i}\times (P_{i,\text{fire},t}+P_{i,\text{wind},t}+P_{i,\text{MT},t}-L_{i,\text{ele},t}-P_{i,\text{P2G},t})]\ge 0 \tag{28}$$

$$0\le\rho_{i,t,\min}\perp(P_{i,\text{DG},t}-P_{i,\text{DG},\min})\ge 0 \tag{29}$$

$$0\le\rho_{i,t,\max}\perp(P_{i,\text{DG},\max}-P_{i,\text{DG},t})\ge 0 \tag{30}$$

where GSF_{l-i} is the generation transfer factor between line nodes l and i.

Because the constraints (27)–(30) are nonlinear terms, the problem is still difficult to solve, so consider linearizing the nonlinear constraints. By introducing auxiliary binary variables, the nonlinear constraint conditions are transformed as follows:

$$\begin{cases} 0\le\pi_{l,t,\min}\le M_{\pi,t,\min}v_{\pi,l,t,\min} \\ P_{\text{ele},l,\lim}+GSF_{l-i}\times(P_{i,\text{fire},t}+P_{i,\text{wind},t}+P_{i,\text{MT},t} \\ \quad -L_{i,\text{ele},t}-P_{i,\text{P2G},t})\le M_{\pi,t,\min}(1-v_{\pi,l,t,\min}) \\ 0\le\pi_{l,t,\max}\le M_{\pi,t,\max}v_{\pi,l,t,\max} \\ P_{\text{ele},l,\lim}-GSF_{l-i}\times(P_{i,\text{fire},t}+P_{i,\text{wind},t}+P_{i,\text{MT},t} \\ \quad -L_{i,\text{ele},t}-P_{i,\text{P2G},t})\le M_{\pi,t,\max}(1-v_{\pi,l,t,\max}) \end{cases} \tag{31}$$

$$\begin{cases} 0\le\rho_{i,t,\min}\le M_{\rho,t,\min}v_{\rho,i,t,\min} \\ P_{i,\text{DG},t}-P_{i,\text{DG},\min}\le M_{\rho,t,\min}(1-v_{\rho,i,t,\min}) \\ 0\le\rho_{i,t,\max}\le M_{\rho,t,\max}v_{\rho,i,t,\max} \\ P_{i,\text{DG},\max}-P_{i,\text{DG},t}\le M_{\rho,t,\max}(1-v_{\rho,i,t,\max}) \end{cases} \tag{32}$$

Among them, $M_{\pi,t,\min}$, $M_{\pi,t,\max}$, $M_{\rho,t,\min}$, $M_{\rho,t,\max}$ are sufficiently large constants; $v_{\pi,l,t,\min}$, $\nu_{\pi,l,t,\max}$, $v_{\rho,i,t,\min}$, $v_{\rho,i,t,\max}$ are the auxiliary binary variables. In this way, the single-level optimization problem becomes a MILP problem, in which we can use the CPLEX solver. The specific process of the above method is shown in Table I.

IV. Case Study

This study used a typical smart district, which included a modified IEEE 9-node power system, 7-node natural-gas system, and a 6-node thermal system for analysis, - see Fig. 3. The transmission capacity limits of branches A-D and B-F are 1,000 kW and 4,000 kW, respectively. The load is evenly distributed among the three load nodes D, E, and F. A wind farm with a rated capacity of 3,600 kW is connected to the system at node C and its quoted price is 8$/MW, contrary to the price for energy surplus, 7$/MW. The quotation price of the two gas wells is 1$/kcf and 1.15$/kcf, respectively.

The electricity, gas, and heat load of the IES and the predicted output curve of the wind farm are shown in Fig. 4. And the energy price of electricity and natural gas are shown in Fig. 5.

A. The Impact of The P2G on The Scheduling Result

Two cases are designed in Fig. 6 to analyze the impact of P2G equipment on the operation of the system: In case 1, P2G is used to absorb wind power on a large scale; In case 2, P2G equipment is not considered.

According to the comparison analysis in Table II and Fig. 6, the wind power utilization rate in case 2 is 92.5%, while increases to 99.6% in case 1, as the reduced curtailment power is

TABLE I
Nonlinear Constraint Linearization Process

1.0	Preparations for nonlinear natural gas constraint linearization
1.1	Piecewise linearization of Weymouth
1.2	Natural gas branch flow analysis
1.3	Introduce auxiliary variables in formulas (3), (4)
2.0	Transform the lower model into the upper model's additional conditions
2.1	Utilize complementary relaxation conditions in KKT conditions in formulas (25), (26)
2.2	Introduce auxiliary variables in formulas (27)–(30)

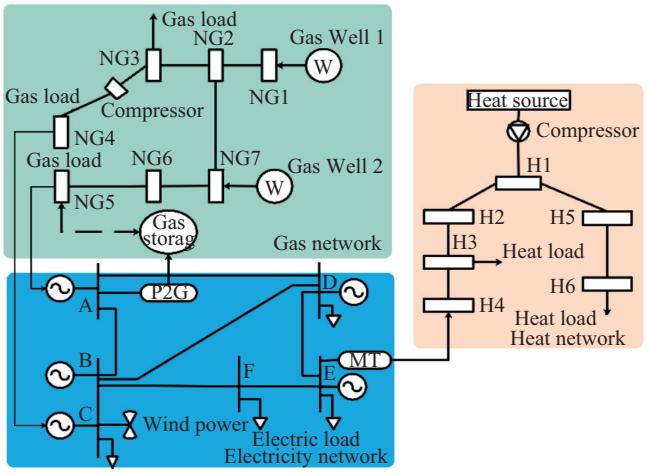

Fig. 3. Schematic of the IEEE 9-node system, 7-node natural-gas system and 6-node thermal system.

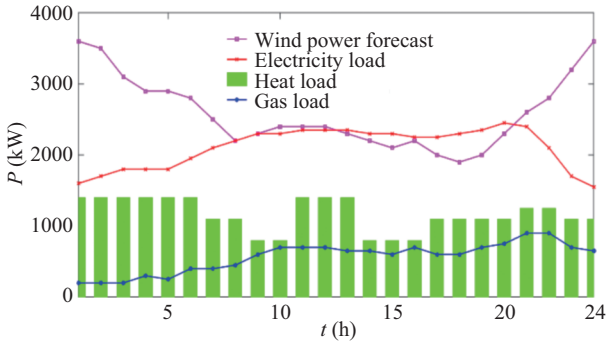

Fig. 4. Electric, heat load and wind-farm forecast output-curve.

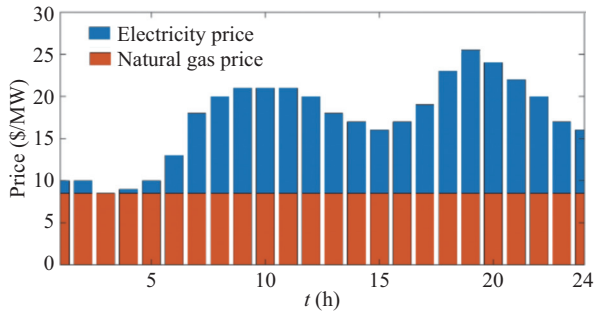

Fig. 5. Electricity price and natural-gas price.

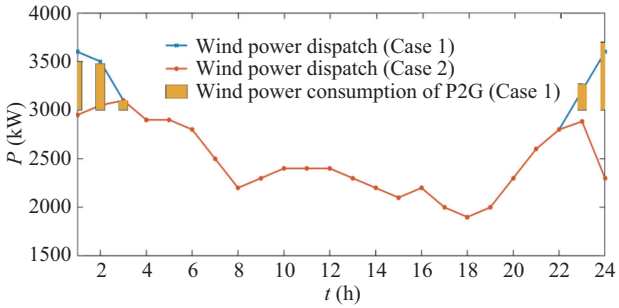

Fig. 6. Comparison of wind power dispatching under different cases.

TABLE II
COMPARISON OF THE SCHEDULING RESULTS FOR THE DIFFERENT SCENARIOS

Case	Upper ($)	Lower ($)	Total ($)	WT (%)	P2G (kcf)
1	13,682	28,783	42,465	99.6%	837.6
2	13,682	29,685	43,367	92.5%	0

consumed by P2G. After comparing the wind power prediction in Fig. 4 and Fig. 6, we can see that the surplus wind-power primarily occurred during periods 0–3 h and periods 23–24 h. For these periods, the system load is relatively low, while wind-power output is high, and the system could not fully absorb all wind power. Therefore, the surplus wind-power in scenario 2 is high. After the introduction of P2G in scenario 1, the surplus wind-power is converted into natural gas via the P2G process during periods 0–3 h and periods 23–24 h. This increased the consumption by the electric load, which is similar to "filling the valley" of the electricity load. Therefore, it could effectively improve the utilization rate of wind power, which confirms that P2G can effectively improve wind-power consumption.

Table II shows that the optimal dispatch costs of top-level natural gas in Scenarios 1 and 2 are the same, and the cost for economic dispatch of the lower-level network in Scenario 2 is higher. This is because the economic dispatch model of the lower-level grid does not consider electricity-to-gas. With higher surplus wind-power and higher costs, the output of gas-fired units remains unchanged, and the gas-supply volume within the natural gas network remains unchanged. Therefore, the top-level natural-gas system has the same operation costs. Furthermore, in scenario 1, because P2G uses surplus wind to produce a certain amount of synthetic natural gas, the reuse of this fraction of natural gas can benefit the IES.

B. The Impact of Surplus Wind-power Costs on Wind-power Utilization

To analyze the impact of surplus costs and coefficients on the wind-power-utilization rate and the process of P2G conversion, the cost-coefficients of surplus costs are calculated from 0 to 10, respectively. The utilization rate of wind power and the electricity load consumed by converting P2G are shown in Fig. 7.

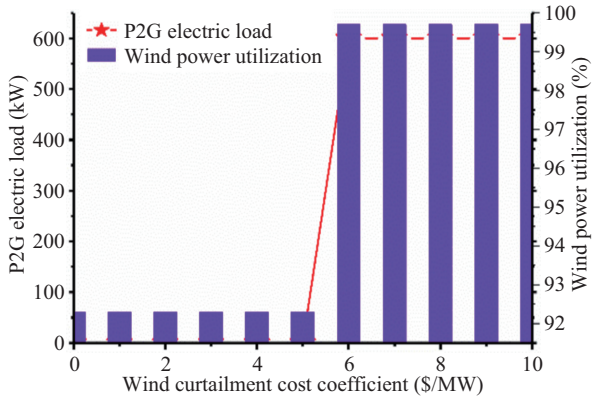

Fig. 7. Wind power utilization rates and consumed power by P2G for different surplus costs.

It can be seen from Fig. 5 that, when the cost of surplus is not considered (the cost-coefficient for surplus is 0), the P2G equipment does not consume electricity, and the wind-power-utilization rate is the same without considering P2G (92.5%), when the cost-coefficient of surplus gradually increases. Within the range of 1 $\sim$ 5, both the wind-power utilization rate and P2G electricity load are the same without considering the cost of wind surplus. In other words, for this cost factor, P2G consumes wind power to generate SNG and lacks economic incentives. When the surplus wind-power cost-coefficient starts to exceed 6, P2G consumes electricity. The reason is that after the wind curtailment cost coefficient is large enough, the total revenue of reducing wind curtailment and P2G synthetic natural gas is greater than or equal to the unit price of wind power. At the same time, the utilization rate of wind power increased to 99.6%, but due to the constraints of P2G capacity, wind power is still not fully absorbed. The capacity of wind power absorption has reached its limit after the wind curtailment cost coefficient reaches 6.

C. Comparison Between Two-layer- and Single-layer-models

The optimal allocation results of the gas well in the two models and the dispatching output results of the MT unit and non-MT unit in the power system are shown in Figs. 8 and 9 respectively. The scheduling results are shown in Table III.

The wind-power-outputs for the two scheduling models are identical but the other obtained scheduling results are significantly different. Figure 8 indicates that, in the dual-layer model, the total gas supply of gas well 1 is 19,673 kcf, which is more than the 13,675 kcf of the single-layer model. The total gas supply of gas well 2 is 25,268 kcf, which is higher than the single-layer model (17,638 kcf). Because the price of gas well 1 is lower than that of gas well 2, the economics of

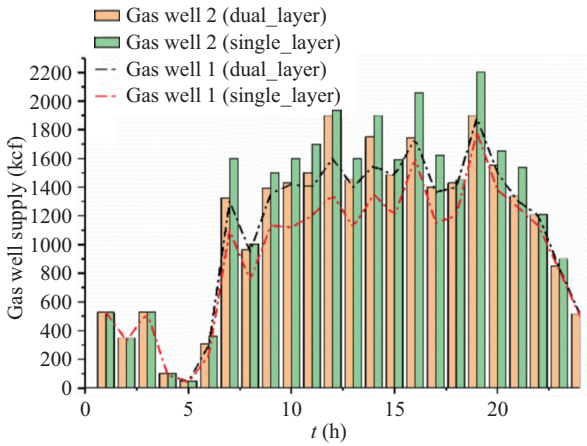

Fig. 8. Gas supply volume for the two models.

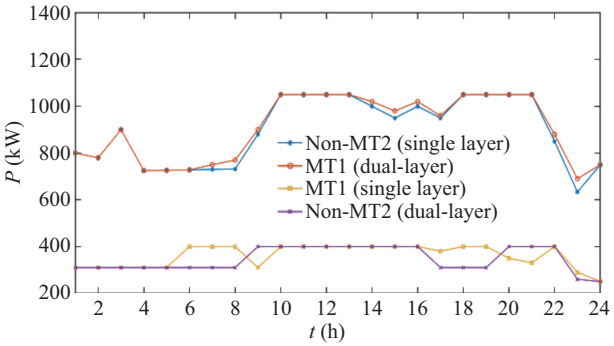

Fig. 9. Comparison of generator dispatch output for the two models.

TABLE III
COMPARISON OF SCHEDULING RESULTS BETWEEN DOUBLE-LAYER MODEL AND SINGLE-LAYER MODEL

Model	Gas system cost ($)	Power system cost ($)	Total cost ($)	Wind power utilization (%)	P2G amount (kcf)
Single	14,278	57,538	71,816	99.5	700.56
Double	13,756	54,643	68,399	99.5	497.68

the natural-gas system are considered independently under the dual-layer model, which can better respond to the quotation of the gas well. Therefore, the cost of the top-layer model in the two-layer model is lower than that in the single-layer model.

Figure 9 shows that the output of units under the two models are different during the dispatch period. The output of non-MT1 under the double-layer model is higher than under the single-layer model, while the price of MT1 is lower. Therefore, the total cost in the double-layer model is smaller than under the single-layer model. For MT2, the total outputs in the double-layer model and the single-layer model are 6,567.68 MW and 6,922.43 MW, respectively. Under the condition of the double-layer model, the total output is less. This is because the output of MT1 increased more, which reduced the output of MT2 with a higher price. The results suggest that the novel two-layer model is reasonably accurate.

V. CONCLUSION

In this paper, taking advantage of the multi-energy complementary characteristics of the P2G and MT, an electric-gas-heat two-layer optimal dispatch model is proposed to absorb the abandoned wind. The upper layer is the natural gas network optimal dispatch model, and the lower layer is the electric-heat network optimal dispatch model. From the simulation analysis, it can be concluded that P2G and MT can significantly absorb excess wind power resources and play a role of "peak shaving and filling valleys" for the electricity network. At the same time, the excess energy is provided to the natural gas network and the thermal network, reducing the operating cost of the total system. Comparing the two-layer model and the single-layer model, the running cost of the two-layer model is lower and the result is more reasonable.

REFERENCES

[1] S. Long, O. Marjanovic, and A. Parisio, "Generalised control-oriented modelling framework for multi-energy systems," *Applied Energy*, vol. 235, pp. 320–331, Feb. 2019.

[2] H. Wang, A. Saint-Pierre, and P. Mancarella, "System level cost and environmental performance of integrated energy systems: An assessment of low-carbon scenarios for the UK," in *Proceedings of 2015 IEEE Eindhoven PowerTech*, Eindhoven, 2015, pp. 1–6.

[3] Y. Gao and Q Ai, "Distributed cooperative optimal control architecture for AC microgrid with renewable generation and storage," *International Journal of Electrical Power & Energy Systems*, vol. 96, pp. 324–334, Jan. 2018.

[4] Y. Gao and Q. Ai, "Distributed multi-agent control for combined AC/DC grids with wind power plant clusters," *IET Generation, Transmission & Distribution*, vol. 12, no. 3, pp. 670–677, Mar. 2018.

[5] S. Clegg and P. Mancarella, "Integrated electrical and gas network flexibility assessment in low-carbon multi-energy systems," *IEEE Transactions on Sustainable Energy*, vol. 7, no. 2, pp. 718–731, Apr. 2016.

[6] B. H. Liu, Q. Y. Lin, T. W. Zheng, L. J. Chen, and S. W. Mei, "Low carbon economic dispatch for multi-energy distribution network with compressed air energy storage system as energy hub," in *2017 36th Chinese Control Conference*, Dalian, China, 2017, pp. 3083–3088.

[7] J. Liu, W. Sun, and G. P. Harrison, "Optimal low-carbon economic environmental dispatch of hybrid electricity-natural gas energy systems considering P2G," *Energies*, vol. 12, no. 7, pp. 1355, Apr. 2019.

[8] Y. Gao, Q. Ai, M. Yousif, and X. Y. Wang, "Source-load-storage consistency collaborative optimization control of flexible DC distribution network considering multi-energy complementarity," *International Journal of Electrical Power & Energy Systems*, vol. 107, pp. 273–281, May 2019.

[9] L. F. Cheng, T. Yu, H. R. Jiang, S. Y. Shi, Z. K. Tan, and Z. Y. Zhang, "Energy internet access equipment integrating cyber-physical systems: concepts, key technologies, system development, and application prospects," *IEEE Access*, vol. 7, pp. 23127–23148, Feb. 2019.

[10] Y. Gao, Q. Ai, X. Y. Wang, and M. Yousif, "Distributed cooperative economic optimization strategy of a regional energy network based on energy cell–tissue architecture," *IEEE Transactions on Industrial Informatics*, vol. 15, no. 9, pp. 5182–5193, Sep. 2019.

[11] Z. H. Lv, W. J. Kong, X. Zhang, D. D. Jiang, H. B. Lv, and X. H. Lu, "Intelligent security planning for regional distributed energy internet," *IEEE Transactions on Industrial Informatics*, vol. 16, no. 5, pp. 3540–3547, May 2020.

[12] J. D. Wei, J. X. Wang, H. Gao, and X. H. Gao, "Optimal operation of micro integrated energy systems considering electrical and heat load classification and scheduling," in *2017 IEEE Conference on Energy Internet and Energy System Integration (EI2)*, Beijing, China, 2017, pp. 1–6.

[13] E. A. M. Ceseña and P. Mancarella, "Energy systems integration in smart districts: robust optimisation of multi-energy flows in integrated electricity, heat and gas networks," *IEEE Transactions on Smart Grid*, vol. 10, no. 1, pp. 1122–1131, Jan. 2019.

[14] Z. Yuan, M. R. Hesamzadeh, and D. R. Biggar, "Distribution locational marginal pricing by convexified ACOPF and hierarchical dispatch," *IEEE Transactions on Smart Grid*, vol. 9, no. 4, pp. 3133–3142, Jul. 2018.

[15] J. S. Giraldo, J. A. Castrillon, J. C. López, M. J. Rider, and C. A. Castro, "Microgrids energy management using robust convex programming," *IEEE Transactions on Smart Grid*, vol. 10, no. 4, pp. 4520–4530, Jul. 2019.
[16] L. N. Ni, W. J. Liu, F. S. Wen, Y. S. Xue, Z. Y. Dong, Y. Zheng, and R. Zhang, "Optimal operation of electricity, natural gas and heat systems considering integrated demand responses and diversified storage devices," *Journal of Modern Power Systems and Clean Energy*, vol. 6, no. 3, pp. 423–437, May 2018.
[17] A. W. Bizuayehu, A. A. S. De La Nieta, J. Contreras, and J. P. S. Catalão, "Impacts of stochastic wind power and storage participation on economic dispatch in distribution systems," *IEEE Transactions on Sustainable Energy*, vol. 7, no. 3, pp. 1336–1345, Jul. 2016.
[18] W. Y. Zheng, Y. H. Hou, and Z. G. Li, "A dynamic equivalent model for district heating networks: formulation, existence and application in distributed electricity-heat operation," *IEEE Transactions on Smart Grid*, vol. 12, no. 3, pp. 2685–2695, May 2021.
[19] W. Y. Zheng and D. J. Hill, "Incentive-based coordination mechanism for distributed operation of integrated electricity and heat systems," *Applied Energy*, vol. 285, pp. 116373, Mar. 2021.
[20] W. J. Huang, W. Y. Zheng, and D. J. Hill, "Distributionally robust optimal power flow in multi-microgrids with decomposition and guaranteed convergence," *IEEE Transactions on Smart Grid*, vol. 12, no. 1, pp. 43–55, Jan. 2021.
[21] W. Y. Zheng, W. C. Wu, Z. G. Li, H. B. Sun, and Y. H. Hou, "A non-iterative decoupled solution for robust integrated electricity-heat scheduling based on network reduction," *IEEE Transactions on Sustainable Energy*, vol. 12, no. 2, pp. 1473–1488, Apr. 2021.
[22] Q. Hu, B. Zeng, Y. Y. Zhang, H. Hu, and W. X. Liu, "Analysis of probabilistic energy flow for integrated electricity-gas energy system with P2G based on cumulant method," in *2017 IEEE Conference on Energy Internet and Energy System Integration (EI2)*, Beijing, China, 2017, pp. 1–6.
[23] Y. F. Li, Y. Du, K. L. Xiang, C. Y. Lin, H. Y. Lin, and Y. Q. Yang, "Planning model of integrated energy system considering P2G and energy storage," in *2019 IEEE 3rd Conference on Energy Internet and Energy System Integration (EI2)*, Changsha, China, 2019, pp. 1246–1251.
[24] F. Yang, X. L. Yuan, H. K. Bai, S. Yin, and H. M. Liu, "Collaborative planning of integrated natural gas and power supply system considering P2G technique," in *2018 China International Conference on Electricity Distribution (CICED)*, Tianjin, China, 2018, pp. 2216–2220.
[25] X. T. Xing, J. Lin, Y. H. Song, Y. Zhou, S. J. Mu, and Q. Hu, "Modeling and operation of the power-to-gas system for renewables integration: a review," *CSEE Journal of Power and Energy Systems*, vol. 4, no. 2, pp. 168–178, Jun. 2018.
[26] J. N. Liu, H. Z. Zhong, K. W. Zeng, H. X. Fan, and Q. X. Chen, "Optimal scheduling of multiple energy system considering power to gas unit," in *2017 IEEE Conference on Energy Internet and Energy System Integration (EI2)*, 2017, pp. 1–6.
[27] S. Clegg and P. Mancarella, "Integrated modeling and assessment of the operational impact of power-to-gas (P2G) on electrical and gas transmission networks," *IEEE Transactions on Sustainable Energy*, vol. 6, no. 4, pp. 1234–1244, Oct. 2015.
[28] H. Khani and H. E. Z. Farag, "Optimal day-ahead scheduling of power-to-gas energy storage and gas load management in wholesale electricity and gas markets," *IEEE Transactions on Sustainable Energy*, vol. 9, no. 2, pp. 940–951, Apr. 2018.
[29] Y. H. Sun, B. W. Zhang, L. J. Ge, D. Sidorov, J. X. Wang, and Z. Xu, "Day-ahead optimization schedule for gas-electric integrated energy system based on second-order cone programming," *CSEE Journal of Power and Energy Systems*, vol. 6, no. 1, pp. 142–151, Mar. 2020.

Yang Gao received a Ph.D. degree at Shanghai Jiao Tong University, Shanghai, China in 2019. After spending one year at KTH Royal Institute of Technology, Sweden, and two years at the University of Manchester, UK, and the University of Bristol, UK, he returned to Shanghai Jiao Tong University. Currently he is an Assistant Professor with the Key Laboratory of Control of Power Transmission and Conversion, Ministry of Education, Shanghai Jiao Tong University, Shanghai, China. His main interests include digital twin optimization and control of integrated energy systems, microgrid, and multi-agent technology in the Energy-internet.

Qian Ai received his Bachelor's degree, Master's degree and Ph.D. degree in Electrical Engineering from Shanghai Jiao Tong University, Wuhan University and Tsinghua University, in 1991, 1994 and 1999, respectively. After spending one year at Nanyang Technological University, Singapore and two years at the University of Bath, UK, he returned to Shanghai Jiao Tong University. Currently he is a Professor with the School of Electronic Information and Electrical Engineering, Shanghai Jiao Tong University, Shanghai, China. His main interests include power quality, load modeling, smart grid, Microgrid and intelligent algorithms.